Thermostability and Irreversible Activity Loss of Exoglucanase/Xylanase Cex from *Cellulomonas fimi*†

Penka V. Nikolova,‡ A. Louise Creagh,‡,§,|| Sheldon J. B. Duff,§,⊥ and Charles A. Haynes*,‡,§,||

Biotechnology Laboratory, UBC Pulp and Paper Centre, Department of Chemical Engineering, and Protein Engineering Network of Centres of Excellence, University of British Columbia, Vancouver, British Columbia, Canada, V6T 1Z3

Received September 19, 1996; Revised Manuscript Received November 21, 1996⊗

ABSTRACT: The activity of the β-1,4-glycanase Cex (EC 3.2.1.91) from *Cellulomonas fimi* is investigated in connection with its industrial application in cellulose hydrolysis and its potential use in cellosaccharide synthesis. Catalytic activity measurements as a function of temperature, complemented with differential scanning calorimetry (DSC) data, are used to characterize the thermostability of the protein and the influence of interdomain interactions. The data suggest that the enzyme is irreversibly deactivated in one of two possible ways: (1) through a low-temperature route characterized by first-order kinetics; or (2) through a high-temperature route characterized by an initial reversible step followed by an irreversible step. Melting temperatures (T_m) of Cex and p-33 (the isolated catalytic domain of Cex) as estimated by DSC are 64.2 and 64.0 °C, respectively, suggesting that the binding and catalytic domains of the protein fold independently. Kinetic parameters (K_m, k_{cat}, and k_{cat}/K_m) of Cex for the hydrolysis of *p*-nitrophenyl β-D-cellobioside (pNPC) were determined at temperatures ranging from 15 to 80 °C. As demanded by reversible mass-action thermodynamics, the T_m of Cex in the presence of excess ligand as determined from activity−temperature data is *ca.* 66.55 °C, more than 2 °C higher than the T_m for Cex under ligand-free conditions. The effect of temperature on the rate constant has been determined using Arrhenius plots. Combined with irreversible deactivation half-life data and DSC data, the results are used to evaluate a model, based on a theory developed by Hei *et al.* (1993), for predicting the time-dependent activity and active-state stability of the protein under a range of potential operating conditions.

The β-1,4-glycanase (Cex)[1] of *Cellulomonas fimi* (EC 3.2.1.91), a mixed xylanase/exoglucanase, is representative of a class of polysaccharidases being investigated by the textile industries and, particularly, the pulp and paper industries, for applications ranging from fabric modification (*e.g.*, "stone-washed"), to dissolving, bleaching, and beating of pulps, to production of biomass energy (Henrissat, 1994; Miller, 1995; Jeffries, 1992). The potential of Cex for synthesis of oligosaccharides by transglycosylation is also being studied (Nikolova *et al.*, 1996). Economical incorporation of an enzymatic step in these industrial processes requires retention of enzymatic activity in liquid environments far from ambient. For example, typical operating conditions for biobleaching 5% consistency birchwood kraft pulp using a xylanase are 65 °C and pH 6.0 (Garg *et al.*, 1996; Jeffries, 1992). Application of a xylanase such as Cex to these processes therefore requires accurate knowledge of enzyme activity as a function of exposure time and solution conditions, particularly temperature, and an understanding of enzyme thermostability in the presence of substrate. In this work, a simple general model, based on the thermodynamic and kinetic subprocesses driving enzyme inactivation, is presented which accounts for the complex dependence of enzyme deactivation on solution conditions and time.

Cex belongs to family X (formerly family F) glycosyl hydrolases and has been subject to numerous investigations. It is a modular protein comprised of 2 discrete structural and functional units, namely, an N-terminal catalytic domain (p-33) and a C-terminal cellulose-binding domain (CBD_{Cex}), joined together by a linker polypeptide consisting of 20 proline and threonine alternating residues (O'Neill *et al.*, 1986). Although a structure for the intact enzyme is not available, high-resolution structures of the isolated catalytic and cellulose-binding domains (Bedarkar *et al.*, 1992; White *et al.*, 1994; Xu *et al.*, 1995) indicate that the linker polypeptide may act to buffer direct interaction of the catalytic domain (p-33) and the binding domain (CBD_{Cex}). However, the extent to which interdomain interactions stabilize or destabilize the active forms of the two domains is not known. In this work, differential scanning calorimetry is used to determine the influence of interdomain interactions

† This work was supported by funds from the Protein Engineering Network of Centers of Excellence of Canada and the Natural Science and Engineering Research Council of Canada (NSERC). P.V.N. is a recipient of an NSERC Postdoctoral Fellowship.

* Author to whom correspondence should be addressed at the Biotechnology Laboratory, 237 Wesbrook Building, University of British Columbia, Vancouver, British Columbua, Canada V6T 1Z3. Phone: (604) 822-5136. Fax: (604) 822−2114. E-mail: israels@chml.ubc.ca.

‡ Biotechnology Laboratory.

§ Department of Chemical Engineering.

|| Protein Engineering Network of Centres of Excellence.

⊥ UBC Pulp and Paper Centre.

⊗ Abstract published in *Advance ACS Abstracts,* January 15, 1997.

[1] Abbreviations: Cex, *Cellulomonas fimi* β-1,4-exoglycanase; CBD_{Cex}, cellulose-binding domain from Cex; p-33, catalytic domain from Cex; pNPC, 4-nitrophenyl β-cellobioside; pNP, 4-nitrophenol; DSC, differential scanning calorimetry; K_{RD}, equilibrium constant for reversible protein unfolding; T_m, melting temperature; E_a and A, activation energy and constant for the Arrhenius equation; k_{di}, first-order rate constant for protein inactivation; k_d, global first-order rate constant for protein inactivation; N, native enzyme; D, reversibly denatured enzyme; $[P_a]_o$, initial enzyme concentration; ΔC_p, change in heat capacity for thermal unfolding; ΔH, change in enthalpy for thermal unfolding; R, universal gas constant; T, absolute temperature.

S0006-2960(96)02367-7 CCC: $14.00

on the stabilities of the binding and catalytic domains of Cex. Some insights can be drawn from the limited data available for organizationally related proteins, which include many xylanases, cellulases, and hemicellulases (Black *et al.*, 1995; Chen *et al.*, 1995; Dominquez *et al.*, 1995; Doolittle, 1995; Gilkes *et al.*, 1991a). Berland *et al.* (1995) report that the unfolding thermodynamics for the granulated starch-binding domain of a two-domain glucoamylase from *Aspergillus niger* are influenced by the presence of the catalytic domain.

No native glycanase has been shown to undergo completely reversible thermal denaturation, making it difficult (without additional information) to convert denaturation enthalpy data obtained from direct thermal denaturation probes such as differential scanning calorimetry (Privalov, 1989) into desired Gibbs energies of denaturation. However, in irreversible denaturation systems which show no scan-rate dependence, Sanchez-Ruiz *et al.* (1988) and others (Edge *et al.*, 1985; Ruiz-Arribas *et al.*, 1994; Iwagami *et al.*, 1995) have proven that kinetically-controlled subprocesses make a negligible contribution to the melting curve and, thus, DSC thermograms can be analyzed by reversible two-state theory to obtain a description of protein stability and unfolding thermodynamics.

Hei and Clark (1993) have shown that direct measurement of enzymatic activity may also provide a potential route to assessing native enzyme stability. Combining kinetic data with two-state theory, they derived a model for predicting initial enzyme activity as a function of solution conditions and then, by implicitly invoking the theory of Sanchez-Ruiz *et al.* (1988), applied it to zero-time kinetics data at elevated temperatures for β-galactosidase from *Escherichia coli*, which denatures irreversibly (Edwards *et al.*, 1990; Hei *et al.*, 1993). This allowed high-temperature enzyme kinetics data to be modeled as a reversible denaturation/inactivation step followed by a first-order irreversible inactivation reaction, although no attempt was made to verify that the T_m was, in fact, scan-rate independent.

Application of enzyme kinetics to thermostability analysis offers several advantages. When present in excess, substrates are known to enhance the thermostability of enzymes in proportion to the Gibbs energy change driving formation of the enzyme−substrate complex (Edge *et al.*, 1985). Thus, the approach allows for direct determination of thermostability in the true processing environment. As noted by Hei *et al.* (1993), activity−temperature measurements can also use cheaper, more readily available equipment, and less pure enzyme than the conventional DSC approach.

The advantage of DSC, however, is that it provides a direct, model-independent measure of the thermodynamic parameters defining thermostability. The kinetic approach is model dependent, and limited data are available with which to evaluate the sensitivity of the model to each model parameter. Thus, the inherent uncertainties associated with using the model to regress these parameters from temperature−activity data are unknown. Moreover, at present, the kinetic approach of Hei *et al.* (1993) has only been applied to inactivation of β-galactosidase, a complex homotetrameric enzyme, which brings the general utility of the approach into question.

In this work, we establish that the theory proposed by Hei and Clark is applicable to Cex inactivation by demonstrating the scan-rate independence of DSC thermograms. The validity and utility of the model are then assessed by comparing, in a thermodynamically consistent manner, regressed thermostability parameters with those directly determined by DSC. Finally, the model is extended to allow for the prediction of irreversible enzyme activity loss as a function of time with the aim of providing a simple methodology for predicting (1) thermostabilities in the presence of substrate and (2) residual activities of enzymes in harsh processing environments. We identify two modes of enzyme inactivation, only one of which involves an initial reversible denaturation step.

EXPERIMENTAL PROCEDURES

Protein Production and Purification. Cex was produced as described by O'Neill *et al.* (1986). The culture was induced for 3 h by addition of isopropyl β-D-thiogalactoside (IPTG) to 0.1 mM final concentration. The cells were harvested by centrifugation, and the total yield amounted to 118 g wet weight of pellet. The cells were pressed with a prechilled (4 °C) French press chamber; phenylmethanesulfonyl fluoride (PMSF), pepstatin A, and EDTA were added to 0.5 mM, 1 mM, and 1 mM, respectively. The cell-free crude extract was centrifuged at 4 °C for 30 min at 15 000 rpm. The supernatant was subjected to further purification according to the protocol of Gilkes *et al.* (1988, 1991b). The final protein fractions were eluted from a 1-L column packed with CF-1 cellulose (Sigma) with distilled water. The absorbance of the eluate was monitored continuously at 280 nm. Desired protein fractions were pooled and centrifuged at 40 000*g* for 30 min. The supernatant was concentrated by diafiltration using an Amicon ultrifiltration unit with a PM 10 membrane. The purity of Cex was assessed by SDS−PAGE and silver staining, using the Fast system and a Pharmacia control unit. The purified-to-homogeneity protein was then subjected to lyophilization and stored at 4 °C for use during the course of these studies. The isolated catalytic domain of Cex was obtained from the wild-type enzyme (purified as described above) by digestion using a *C. fimi* protease, followed by gel filtration chromatography (Gilkes *et al.*, 1988, 1991b).

Determination of the Protein Concentration. The concentrations of purified protein samples were determined by UV spectroscopy at 280 nm. The extinction coefficient at 280 nm of a 1 mg·mL^{-1} sample in a 1 cm cuvette was previously estimated to be 1.61 (Gilkes *et al.*, 1992) and used in the calculations throughout this study.

Kinetic Studies. Kinetic studies were made by monitoring the changes in absorbance using a Pye Unicam PU-8800 spectrophotometer equipped with a temperature-controlled water bath. The hydrolysis of *p*-nitrophenyl β-D-cellobioside (Sigma Chemicals) was monitored as previously reported by Kempton and Withers (1992). Initial reaction rates were measured for 7−10 different substrate concentrations, ranging from 0.2 to 10 times K_m in 50 mM potassium phosphate buffer, pH 7.0, at constant temperature in 1 cm cuvettes, which were thermally equilibrated within the heating block of the spectrophotometer. The temperature of the reaction mixture was monitored throughout the course of the assays by inserting a temperature probe in the cuvettes. Reactions were initiated by the addition of enzyme, and the release of the product (*p*-nitrophenol) was monitored at 400 nm continuously. The substrate pNPC was stable at all temperatures. No background (spontaneous) hydrolysis was

detected at any reaction condition under investigation. Extinction coefficients for the product were determined from standard curves prepared at each reaction temperature at which kinetic parameters were determined. The extinction coefficient, ϵ at 400 nm for *p*-nitrophenol, varied linearly with temperature over the entire temperature range. Michaelis−Menten parameters were determined by nonlinear regression analysis using the software GraFit (Leatherbarrow, 1990). All measurements were done in triplicate or higher.

Determination of Residual Enzyme Activity as a Function of Temperature. Thermal effects on enzyme activity were determined across the temperature range of 37−75 °C. Ligand-free enzyme samples were incubated in a temperature-controlled water bath, and aliquots were taken during different time intervals and cooled on ice to room temperature. Residual enzyme activity data for the hydrolysis of pNPC were determined at constant temperature (37 °C) as described above.

Differential Scanning Calorimetry (DSC). Calorimetric measurements were performed using a Calorimetry Sciences Corp. Model 7707 differential scanning calorimeter. Thermograms were measured for 0.5 mL samples containing 2.0 mg/mL protein in 50 mM buffer, at a scan rate of 1 °C min^{-1}. All samples were prepared by exchanging using an Amicon ultrafiltration cell with a 10 kDa MW cutoff membrane the 50 mM KP_i buffer in which protein sample was stored with one of the following 50 mM buffers: acetate (pH 4.5), NaP_i (pH 6.03, 7.42, 7.75, 8.1, 8.7), and glycine−NaOH (pH 9.02). The final buffer eluted from the ultrafiltration cell was used as reference buffer in the DSC experiments. A background scan with the reference buffer in both the sample and reference cells was subtracted from the scans recorded for the protein sample. The change in heat capacity upon denaturation, ΔC_p, was determined from DSC thermograms at various pHs (Liu & Sturtevant, 1996; Wintrode *et al.*, 1995). ΔH was found to vary linearly with temperature between pH 6 and 9. Below pH 5.5, the protein precipitates during denaturation, making it impossible to deconvolute the denaturation thermogram. The reversibility of protein unfolding was evaluated by rescanning the samples immediately after cooling from the first heating cycle (Thello-Solis & Hernandez-Arana, 1995). All experiments were done in duplicate.

Curve Fitting. Nonlinear regression analysis using a Levenberg−Marquardt curve-fitting algorithm (Origin Software Co.) was applied to the experimental data in conjunction with eqs 1−3 describing the effect of temperature on the equilibrium constant (K_{rd}), and thus v_o. The Arrhenius plot (Figure 3) was used to calculate the activation energy, E_a, and the Arrhenius constant, A, for catalysis according to eq 2. The values for ΔC_p and ΔH were determined from DSC thermograms for Cex in a ligand-free environment. The value of T_m in the presence of ligand was then regressed from kinetic data as a function of temperature using the nonlinear theory described under Results and Discussion with ΔH and ΔC_p fixed at the values determined from calorimetry.

RESULTS AND DISCUSSION

DSC Thermograms and Domain Stability Analysis. Figure 1 shows the DSC thermogram for Cex (47 kDa) at pH 7.0 (50 mM phosphate buffer). The thermodynamic observables in a single DSC thermogram are the denaturation temperature

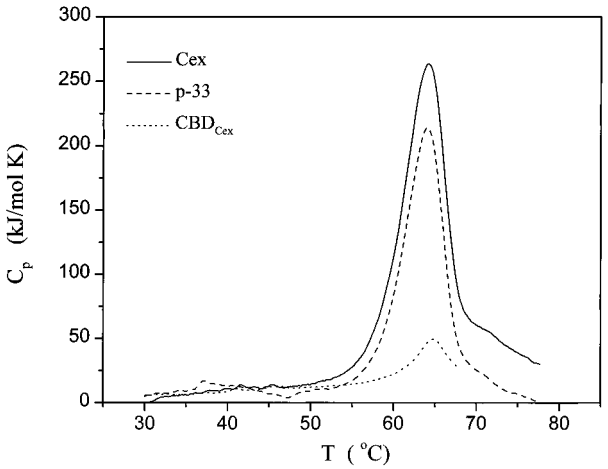

FIGURE 1: Differential scanning calorimetry thermograms for Cex (solid line), p-33 (dashed line), and CBD_{Cex} (dotted line) at pH 7.0 and a scan rate of 1 °C min^{-1}. Protein concentration: 1 mg mL^{-1} in 50 mM potassium phosphate buffer.

Table 1: Kinetic Parameters for β-1,4-Exoglucanase Cex or Catalytic Domain p-33 Catalyzed Hydrolysis of pNPC at 37 °C in 50 mM Potassium Phosphate Buffer, pH 7.0[a]

Michaelis−Menten constants	Cex	p-33
K_m (mM)	0.70	0.51
k_{cat} (s^{-1})	5.60	11.81
k_{cat}/K_m (s^{-1} mM^{-1})	8.00	23.15

[a] Calculation of the kinetic constants for Cex and p-33 is based on the experimental masses as determined by mass spectrometry. The masses of Cex and p-33 are 47 107 and 35 488 Da, respectively. CBD_{Cex} has a mass of 10 918 Da.

T_m, the change in enthalpy ΔH for thermal unfolding of the protein at T_m, and, for sufficiently precise data, the heat capacity change ΔC_p for denaturation. In general, ΔC_p is regressed from $\Delta H(T)$ data rather than from a single DSC thermogram. Cex denatures irreversibly without precipitation between pH 6 and 9. Thermograms immediately following the initial denaturation scan were essentially void of the endothermic peak characteristic of the native to denatured state transition, although partial reversibility could be observed under certain conditions. The T_m for Cex at pH 7.0 is 64.2 (±0.2) at a scan-rate of 1 °C min^{-1}, and remains at that value with changing scan-rate over the range 0.5−1.3 °C min^{-1}. Thus, the mechanistic arguments derived by Sanchez-Ruiz *et al.* (1988) are applicable to the description of Cex inactivation at elevated temperatures.

Table 1 reports measured Michaelis−Menten catalytic constants for hydrolysis of pNPC by Cex and p-33 at 37 °C and pH 7. Removal of the binding domain leads to a small but significant enhancement in the catalytic activity, as evidenced by the increase in k_{cat}/K_m, which suggests that interdomain interactions may influence the catalytic activity of Cex (Tomme *et al.*, 1995). There are examples where isolation of the catalytic region of a multidomain enzyme does not significantly alter catalytic activity but does cause a substantial reduction in domain stability (Tanaka *et al.*, 1995; Terashima *et al.*, 1994; Esen, 1993). For instance, deletion of the N-terminal noncatalytic domain of endoxylanase A (family X) from *T. saccharolyticum* or that of amylopullalanase from *Thermoanaerobacter ethanolicus* results in active enzymes with substantially reduced stabilities measured as decreases in T_m (Lee *et al.*, 1993).

Table 2: Model Parameters Determined from Differential Scanning Calorimetry Thermograms (T_m, ΔH, and ΔC_p) or Regressed from Activity−Temperature Data (T_m^*, ΔH^*, and A and E_a for k_{cat})

model parameter	value
T_m (°C)	64.0 (±0.3)
ΔH (kJ mol^{-1})	1380 (±50)
ΔC_p (kJ mol^{-1} K^{-1})	24.6 (±2.8)
A (μmol min^{-1} mg^{-1})	1.36×10^5 ($\pm 0.1 \times 10^5$)
E_a (kJ mol^{-1})	25.9 (±0.1)
T_m^* (°C)	66.6 (±0.4)
ΔH^* (kJ mol^{-1})	1430 (±80)

When the thermal stabilities of distinct domains within a protein differ significantly, DSC can be used to determine the thermodynamic parameters defining the unfolding transition of each domain (Doolittle, 1995; Ruiz-Arribas *et al.*, 1994). However, the two-domain structure of Cex is not clearly resolved in the DSC thermogram at pH 7 (Figure 1) or at any other pH considered (pH 4.5−10.8; thermograms not shown). The unimodal, Gaussian-type denaturation peak for Cex indicates either that the two domains interact sufficiently to cause cooperative unfolding or that both domains of the intact enzyme denature independently at approximately the same temperature. Combined with DSC data for the two isolated domains, the unimodal denaturation peak for Cex therefore provides a method for qualitatively assessing the influence of interdomain interactions on the stabilities of the catalytic and binding domains in Cex. If interdomain interactions significantly increase or decrease the stability of either domain, we would expect to see differences between the melting temperatures of the individual domains (p-33 and CBD_{Cex}) relative to that measured for Cex.

Figure 1 shows DSC thermograms at pH 7.0 for the isolated domains of Cex. The melting temperatures for p-33 and CBD_{Cex} are 64.0 (±0.2) °C and 64.7 (±0.2) °C, respectively. Thus, both T_m values fall near the midpoint of the denaturation peak for Cex, suggesting that neither domain significantly influences the stability of the other and, thus, that any interactions between the catalytic and binding domains in Cex are weak if present.

Stronger verification of the lack of significant interdomain interactions between p-33 and CBD_{Cex} is provided by the additivity of the denaturation enthalpy ΔH, which (along with the denaturation entropy) is the thermodynamic state function most sensitive to perturbations in stability caused by environmental changes. ΔH values in kJ/mol for p-33 and CBD_{Cex} denaturation at pH 7 are 1020 (±50) and 380 (±40), respectively, which, within experimental error, sum to the molar denaturation enthalpy for Cex (Table 2).

Molecular (relaxation) mechanics calculations using the CHEM3D molecular modeling analysis software (Cambridge Scientific) on the isolate proline-threonine linker region (PT box) free in solution suggest that it folds into an extended helix configuration with a linear fluid structure (Koska, 1996). This leads to a proposed Cex structure where the catalytic and binding domains are separated by the PT box by a linear distance of 4−6 cellobioside units, or about half that predicted assuming the PT box is in a linear conformation (Miller, 1995). A similar structural organization has been reported by Chen *et al.* (1995) for glucoamylase GAI from *Aspergillus awamori*, which has an identical primary sequence to that of *A. niger*. The authors report that deletion of 103 C-terminal residues from GAI, which gives GAII, does not affect enzyme activity on soluble starch or the thermostability of the enzyme, pointing toward the independence of the catalytic from the starch-binding domain.

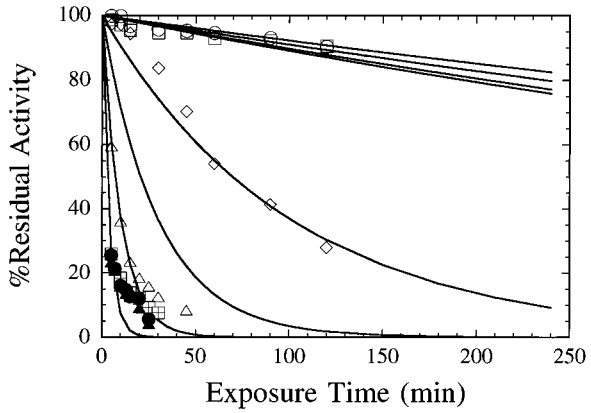

FIGURE 2: Activity−temperature data for hydrolysis of pNPC by β-1,4-exoglucanase/xylanase Cex from *C. fimi* in 50 mM potassium phosphate buffer, pH 7.0: (○) 37 °C; (□) 50 °C; (◇) 55 °C; (△) 61 °C; (plus sign in open box) 66 °C; (●) 70 °C; (▲) 75 °C. Solid curves show model calculations (eqs 2 through 6) at the following temperatures (from top to bottom curve): 0 °C, 20 °C, 40 °C, 50 °C, 60 °C, 61 °C, 63 °C, 65 °C. Model parameters are listed in Tables 2 and 3.

Time- and Temperature-Dependent Inactivation. Figure 2 reports the percent residual activity of Cex as a function of exposure time to solutions (pH 7.0) at set temperatures ranging from 37 to 75 °C. The data represent measured Cex activities at 37 °C following incubation of the enzyme in the substrate-free solution at the specified conditions. Thus, the residual activities in Figure 2 are a measure of the native enzyme and reversibly denatured enzyme which reverts to the native state upon cooling to 37 °C. Only that portion of the enzyme pool which is irreversibly inactivated contributes to the observed loss in activity.

At all temperatures, a simple first-order decay model provides a good description of the irreversible enzyme deactivation kinetics. Gradual inactivation over time is observed at temperatures of 50 °C and below. Between 50 and 66 °C, the rate of inactivation increases rapidly with increasing temperature. At 70 °C and above, the inactivation curves become essentially indistinguishable, all indicating that Cex activity drops to near zero in *ca.* 30 min. First-order decay of enzyme activity is commonly observed (Fontes *et al.*, 1995; Kreimer *et al.*, 1995; Yang *et al.*, 1994; Ray *et al.*, 1994). Moreover, although little interpretation has been provided, a number of studies have also observed decay curves which depend on temperature in a strong, nonlinear manner (Aguado *et al.*, 1995; Eijsink *et al.*, 1995; Wakarchuk *et al.*, 1994).

A first-order deactivation rate constant k_d was regressed at each temperature and plotted in Figure 3 as ln k_d versus reciprocal temperature. The temperatures obtained from the DSC thermogram for Cex (Figure 1) which represent the onset (>99.99% native Cex), midpoint (50% native Cex), and completion of denaturation (<0.01% native Cex) are also indicated in Figure 3 as N, T_m, and D, respectively. Three regimes defined by (1) $T < N$, (2) $N < T < D$, and (3) $T > D$ are observed. In region 1, a gradual irreversible loss in Cex activity is observed which, at any temperature within the region, is significantly greater than the maximum rate

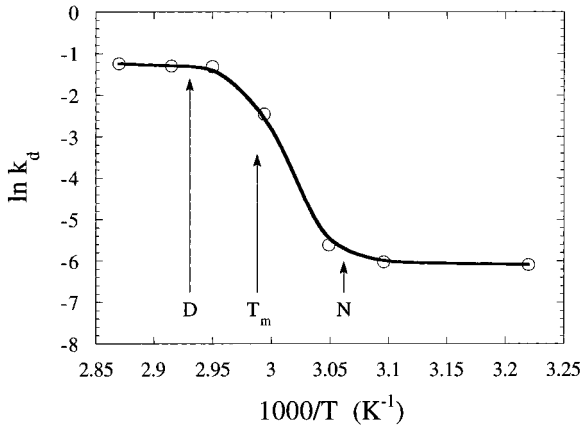

FIGURE 3: Global rate constant of deactivation k_d (s^{-1}) data for Cex as a function of inverse temperature. The temperatures obtained from Figure 1 which represent the onset (>99.99% native Cex), midpoint (50% native Cex), and completion of denaturation (<0.01% native Cex) are also indicated as *N*, T_m, and *D*, respectively.

of deactivation calculated from the value of the equilibrium constant K_{RD} for the native to denatured state transition assuming all reversibly denatured protein is converted to an irreversibly denatured form. Thus, at low temperatures, there is a slow reaction causing irreversible deactivation that does not proceed through a reversibly denatured protein state.

In region 2, this slow reaction is quickly competed out by irreversibly inactivated protein formed from reversibly denatured protein. Finally, at very high temperatures (region 3), essentially all inactive protein is formed from reversibly denatured protein.

Irreversible Inactivation Model Development. The inactivation regimes identified in Figure 3 suggest that the total rate of irreversible inactivation of Cex can be represented by the following reaction scheme:

$$I_1 \xleftarrow{k_{d1}} N \xleftrightarrow{K_{RD}} D \xrightarrow{k_{d3}} I_3 \qquad (1)$$

where N is the native (active) state, D is the reversibly denatured state, and I_1 and I_3 are irreversibly inactivated states. The reaction leading to I_1 represents the low-temperature (regime 1) inactivation of Cex and is characterized by a first-order rate constant k_{d1} (min^{-1}). Formation of I_3 follows a two-step mechanism involving an initial reversible denaturation reaction described by an equilibrium formation constant K_{RD}, where $K_{RD} = [D]/[N]$, followed by an irreversible conversion of D to I characterized by the first-order rate constant k_{d3}.

The total rate of irreversible inactivation can therefore be defined as follows:

$$-\frac{d[P_a]}{dt} = -\frac{d([N] + [D])}{dt} = \frac{d[I_1]}{dt} + \frac{d[I_3]}{dt} \qquad (2)$$

where $[P_a]$ is the total enzyme concentration which can be converted to N upon cooling to 37 °C. Assuming the reversible denaturation of N to D is much faster than the conversion of D to I_3, we can use eq 2 to define a global psuedo-first-order rate constant k_d in terms of K_{RD} and the individual rate constants k_{d1} and k_{d3}:

$$k_d(T) = \frac{k_{d3}K_{RD} + k_{d1}}{1 + K_{RD}} \qquad (3)$$

Table 3: Arrhenius Parameters for Inactivation Rate Constants k_{d1} and k_{d3}

rate constant	E_a (kJ mol^{-1})	A (min^{-1})
k_{d1}	7.6 (±0.3)	3.9 (±0.3)
k_{d2}	5.3	8.3×10^{-3}

The validity of this assumption is based on two observations. First, DSC thermograms for Cex denaturation are scan-rate independent. Second, half-lifes, $t_{1/2}$ (min), of native Cex calculated from the data in Figure 2 are between 305.3 min (37 °C) and 2.4 min (75 °C), and are therefore far slower than forward rate constants for reversible protein unfolding, where typical values range from 1 μs to 10 ms (Shortle *et al.*, 1996).

Comparison of eq 3 with Figure 3 shows that $k_d(T)$ has the correct high- and low-temperature limits. Within region 1, K_{RD} is near zero, and $k_d(T)$ reduces to k_{d1}, while at very high temperatures (region 3) $k_d(T)$ is equal to k_{d3} since K_{RD} is near infinite. The solution of eq 2 for the time dependence of $[P_a]$, where $100 \times ([P_a]/[P_a]_o)$ represents the percent residual activity of the enzyme, assuming k_d is given by eq 3 is

$$[P_a] = [P_a]_o \exp\{-k_d(T)t\} \qquad (4)$$

where t is time and $[P_a]_o$ is the active enzyme concentration at t equals zero.

The global rate constant $k_d(T)$ shows a linear dependence on temperature at the high- and low-temperature limits, indicating that the temperature dependencies of k_{d1} and k_{d3} are well described by the Arrhenius equation:

$$k_i(T) = A_i \exp\left(-\frac{E_{ai}}{RT}\right) \qquad (5)$$

where both A and E_a are temperature independent; values of the Arrhenius constant and activation energy for k_{d1} and k_{d3} are given in Table 3.

The variation in K_{RD} within the van't Hoff envelope accounts for the strong nonlinear temperature dependence of $k_d(T)$ seen in region 2 of Figure 3. Based on the reversible two-state unfolding theories of Privalov (1979), the functional dependence of K_{RD} on temperature is given by (Hei *et al.*, 1993):

$$K^*_{RD}(T) = \exp\left(\frac{\Delta H^*}{RT^*_m} - \frac{\Delta C_p{}^*}{R}(1 + \ln T^*_m) + \left(\frac{\Delta C_p{}^* T^*_m}{R} - \frac{\Delta H^*}{R}\right)\frac{1}{T} + \frac{\Delta C_p{}^*}{R}\ln T\right] \qquad (6)$$

where, the superscript asterisk indicates that the equilibrium applies to the condition where excess substrate is present. Application of eq 6 to irreversible protein inactivation systems is strictly valid for only those systems in which the reversible exchange between N and D is fast compared to the irreversible turnover of D to I_3.

Substrate-Enhanced Thermostability Analysis. The temperature dependencies of the Michaelis−Menten kinetic parameters k_{cat} and K_m were determined with the aim both of better understanding thermal effects on Cex stability and function and of providing an appropriate data set for testing the model proposed by Hei *et al.* (1993). No variation in

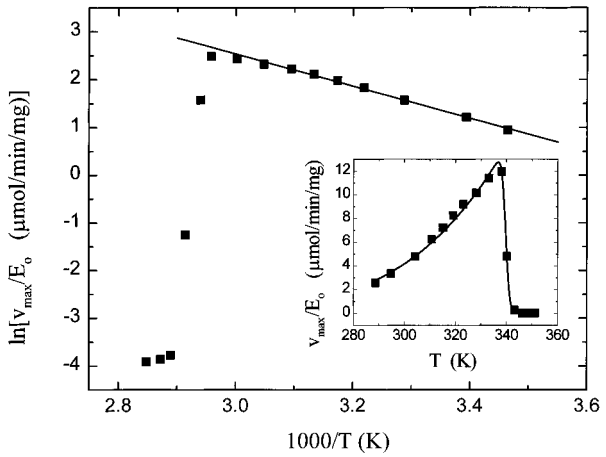

FIGURE 4: Temperature dependence in Arrhenius form of v_{max}/E_o for hydrolysis of pNPC by β-1,4-exoglucanase/xylanase Cex from *C. fimi* in 50 mM potassium phosphate buffer, pH 7.0. Temperature range: 15−78 °C. The regressed Arrhenius parameters and melting temperature T_m^* are given in Table 2. Inset: Activity−temperature plot of the above data. Solid curve calculated by eq 7 with T_m^* and the Arrhenius kinetic parameters regressed to the experimental data (ΔH and ΔC_p taken from independent DSC data).

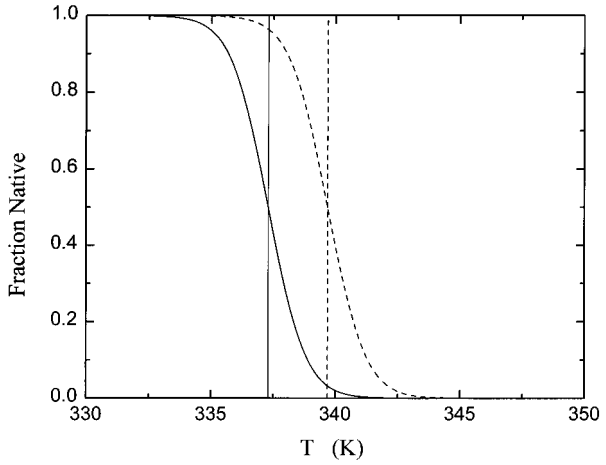

FIGURE 5: Melting curves at pH 7.0 for β-1,4-exoglucanase/xylanase Cex from *C. fimi* in 50 mM potassium phosphate buffer (solid curve) as calculated from the DSC thermogram in Figure 1, and in 50 mM potassium phosphate buffer containing excess pNPC (dashed curve) as calculated from activity−temperature data. Solid and dashed vertical lines indicate the melting temperatures T_m and T_m^*, respectively.

K_m with temperature was observed. Figures 4 and 5 show initial activity data for hydrolysis of pNPC by Cex in linearized form according to the Arrhenius equation and as a function of temperature, respectively, over the range 15−79 °C. The logarithmic form of eq 5 was used to regress the values of A and E_a for k_{cat} from the linear low-temperature portion ($T \leq 50$ °C) of Figure 4; A and E_a are 1.36×10^5 s^{-1} and 25.9 kJ mol^{-1}, respectively, with a linear correlation coefficient r^2 of greater than 0.99.

As shown in Figure 4, Cex activity reaches a maximum at *ca.* 65 °C and then quickly falls to undetectable levels with increasing temperature. The solid line in Figure 4 represents the Arrhenius equation fit to the kinetic data at lower temperatures where the concentration of denatured protein is near zero. The difference between the Arrhenius line extrapolated to high temperatures and the experimental data therefore provides a method for determining the fraction of native enzyme as a function of temperature, from which we can determine T_m^* and $K_{RD}^*(T)$, the denaturation temperature and native-denatured equilibrium constant, respectively, in the presence of substrate at a concentration 10 times K_m. The resulting denaturation curve [K = (100 − % native)/% native] and melting temperature are shown in Figure 5, which presents analogous data for the ligand-free system for comparison. For our mechanistic argument that high-temperature enzyme inactivation proceeds through a reversibly denatured state in which conversion between N and D is fast compared to the turnover to I_3 to be valid, the T_m of the enzyme must increase in the presence of excess substrate (under otherwise constant conditions) due to the chemical potential gradient driving formation of the enzyme−substrate complex (Fukada *et al.*, 1983; Edge *et al.*, 1985; Creagh *et al.*, 1996a). As shown in Figure 5, T_m^* is 2.6 ± 0.4 °C higher than T_m when $[S]/K_m$ equals 10. Increases in T_m of 5−10 °C have been observed at similar $[S]/K_m$ values in systems where the substrate binds tightly to the enzyme (Edge *et al.*, 1985; Fukada *et al.*, 1983). The relatively modest increase of 2.6 °C seen here suggests that pNPC does not bind with high affinity, which is consistent with the measured K_m of 0.7 mM.

Under excess substrate S conditions such that $[S] \gg K_m$, the initial rate v_o for a single enzyme−single substrate reaction is given by

$$v_o = k_{cat}(T)[N] = \frac{k_{cat}(T)[P_a]_o}{1 + K_{RD}(T)} \qquad (7)$$

where the temperature dependencies of k_{cat} and K_{RD} are given by eqs 5 and 6, respectively. The solid curve in the inset of Figure 4 is calculated using eq 7 which assumes that the concentrations of I_1 and I_3 are zero. The correlation between model and experiment is good (A and E_a for k_{cat} and T_m^* are regressed to the data; ΔH and ΔC_p are independent data taken from the DSC analysis).

Direct regression of the enthalpy change (denoted as ΔH^*) to the activity−temperature curve in the inset of Figure 4 gives a value of 1430 ± 80 kJ mol^{-1}. Thermodynamic analysis of ligand binding shows that ΔH^* is equal to ΔH (in the absence of ligand) plus the additional enthalpy ($-\Delta H_b$) required to dissociate the ligand−enzyme complex (Creagh *et al.*, 1996b; Edge *et al.*, 1985). Binding of sugars and sugar analogues to enzymes or to sugar-binding proteins is an exothermic process in which ΔH_b generally lies between −10 and −100 kJ mol^{-1} (Tomme *et al.*, 1996; Sigurskjold *et al.*, 1992). Thus, ligand dissociation should increase ΔH by 10−100 kJ mol^{-1}. In our system, ΔH^* is on average *ca.* 50 kJ mol^{-1} higher than ΔH, although the errors associated with both the measured (ΔH) and regressed values make it difficult to draw any firm quantitative conclusions.

The similarity of ΔH and ΔH^* and their relative magnitudes does, however, validate the potential use of eqs 5−7 and temperature−activity data as a reasonably accurate and inexpensive probe of protein stability in the presence of substrate. As shown in Figure 5, the analysis correctly predicts that the denaturation temperature will increase in the presence of substrate. Theory indicates that the magnitude of this increase is proportional to the logarithm of the substrate-binding constant. As a result, an excess of tight-binding substrate can shift the temperature where maximum activity is observed (*i.e.*, the maximum in Figure 4) to values equal to or greater than the denaturation temperature of the

enzyme in the absence of substrate. DSC is not in general applicable to such studies since the time required to complete a thermogram (usually *ca.* 75 min) far exceeds that required to complete the reaction.

What remains is to establish the accuracy of the kinetic data required to regress meaningful values of T_m^*, ΔH^*, and ΔC_p^*, which together define the themostability of the enzyme in the presence of substrate. The covariance matrix for equilibrium constants calculated with eq 6 indicates that $K_{RD}^*(T)$ is, within model uncertainty, insensitive to ΔC_p^* over the range of possible ΔC_p^* values (0 to *ca.* 40 kJ mol^{-1} K^{-1}) as determined from the extrema of heat capacity data reported in the literature (Wintrode *et al.*, 1995; Liu & Sturtevant, 1996; Privalov, 1979); that is, a ±40 kJ mol^{-1} K^{-1} change in ΔC_p^* does not produce a statistically meaningful change in $K_{RD}^*(T)$. Thus, a single temperature−activity curve cannot be used to regress a true value of ΔC_p^*. In principal, however, an accurate value of ΔC_p^* could be determined from activity-temperature data as a function of pH, from which a plot of ΔH^* versus T_m^* could be constructed. This approach is analogous to that used to regress ΔC_p from calorimetry data.

Both T_m^* and ΔH^* can be regressed with inherent uncertainties derived from covariance analysis of 0.07 °C and 40 kJ mol^{-1}. However, analogous to DSC analysis, their values, particularly ΔH^*, can be in error if any model assumption is violated or the activity−temperature data at the specified pH are inaccurate or of insufficient quantity, particularly in the nonlinear region of the Arrhenius-type plot. Privalov (1979) and Pace (1990) have measured and compiled $\Delta H(T_m)$ data for a large number of reversibly unfolded proteins; values range from 4 to 12 cal g^{-1}, with the vast majority of proteins having a specific ΔH^* between 7 and 9 cal g^{-1}. The ΔH^* regressed in this study equates to a specific value of 7.3 cal g^{-1}, indicating that the basic model proposed by Hei and Clark and extended in this work can yield accurate results under appropriate conditions.

Inactivation Model Calculations. The utility of this methodology can now be demonstrated by applying eqs 3 through 6 and the thermostability model of Hei *et al.* (1993) to the prediction of time-dependent percent residual activities of Cex as a function of temperature such as those shown in Figure 2. In principal, the calculation requires values for the three thermostability parameters T_m^*, ΔH^*, and ΔC_p^*. The first two parameters are given by our temperature-activity analysis. ΔC_p^* is not known, but we have shown that $K_{RD}^*(T)$ is insensitive to the value of ΔC_p^*. Thus, ΔC_p^* was set equal to ΔC_p for all model calculations.

Isothermal inactivation curves calculated with the model equations are shown as a function of time in Figure 2. The model calculations at low (0−50 °C) and high (66−75 °C) temperatures are, in a strict sense, correlations, since k_{d1} and k_{d3} are regressed to those data sets, respectively. However, model calculations between 50 and 66 °C are pure predictions. The model calculations are in good agreement with experiment at all temperatures. Most importantly, the model correctly captures the very strong temperature dependence of the inactivation curves within the reversible denaturation envelope.

CONCLUSIONS

Incorporation of the novel approach of determining enzyme thermostability in the presence of substrate developed by Hei and Clark (1993) into the Cex inactivation model developed here therefore provides an accurate method for predicting the thermostabality and inactivation kinetics of Cex. Given the generality of the approach, it seems reasonable to assume that it could be applied to a wide number of industrially relevant enzymes and processing conditions. However, it will not be appropriate for all systems, only those where one can establish that the reversible denaturation of protein is fast compared with the rate of the subsequent irreversible inactivation step.

ACKNOWLEDGMENT

We thank Drs. R. Antony J. Warren (University of British Columbia), Douglas Kilburn (UBC), Stephen G. Withers (UBC), and David Wilson's laboratory (Alberta Research Council) for their advice and support.

REFERENCES

Aguado, J., Romero, M. D., Rodriguez, L., & Callas, J. A. (1995) *Biotechnol. Prog. 11*, 104−106.
Bedarkar, S., Gilkes, N. R., Kilburn, D. G., Kwan, E., Rose, D. R., Miller, R. C., Jr., Warren, R. A. J., & Withers, S. G. (1992) *J. Mol. Biol. 228*, 693−695.
Berland, C. R., Sigurskjold, B. W., Stoffer, B., Frandsen, T. P., & Svensson, B. (1995) *Biochemistry 34*, 10153−10161.
Black, G. W., Hazlewood, G. P., Millward, Saddler, S. J., Laurie, J. I., & Gilbert, H. J. (1995) *Biochem. J. 307*, 191−195.
Chen, L., Coutinho, P. M., Nikolov, Z., & Ford, C. (1995) *Protein Eng. 8*, 1049−1055.
Creagh, A. L., Ong, E., Jervis, E., Kilburn, D. G., & Haynes, C. A. (1996a) *Proc. Natl. Acad. Sci. U.S.A. 93*, 12229−12234.
Creagh, A. L., Tomme, P., Kilburn, D. G., & Haynes, C. A. (1996b) Protein Engineering Network of Centres of Excellence Annual Meeting, May 5, Montreal, Canada.
Dominquez, R., Souchon, H., Spinelli, S., Danter, Z., Wilson, K. S., Chanvaux, S., Beguin, P., & Alzari, P. M. (1995) *Nat. Struct. Biol. 2*, 569−576.
Doolittle, R. F. (1995) *Annu. Rev. Biochem. 64*, 287−314.
Edge, V., Allewell, N. M., & Sturtevant, J. M. (1985) *Biochemistry 24*, 5899−5906.
Edwards, R. A., Jacobson, A. J., & Huber, R. E. (1990) *Biochemistry 29*, 11001−11008.
Eijsink, V. G. H., Veltman, O. R., Aukema, W., Vriend, G., & Venema, G. (1995) *Struct. Biol. 2*, 374−379.
Esen, A., & Gungor, G. (1993) in *β-Glucosidases: Biochemistry and molecular biology* (Esen, A., Ed.) pp 214−238, ACS Symposium Series, Washington.
Fontes, C. M. G. A., Hazlewood, G. P., Morag, E., Hall, J., Hirst, B. H., & Gilbert, H. J. (1995) *Biochem. J. 307*, 151−158.
Fukada, H., Sturtevant, J, M., & Quiocho, F. A. (1983) *J. Biol. Chem. 258*, 13193−13198.
Garg, A. P., McCarthy, A. J., Roberts, J. C. (1996) *Enzyme Microb. Technol. 18*, 261−267.
Gilkes, N. R., Warren, R. A. J., Miller, R. C., Jr., & Kilburn, D. G. (1988) *J. Biol. Chem. 263*, 10401−10407.
Gilkes, N. R., Henrissat, B., Kilburn, D. G., Miller, R. C., Jr., & Warren, R. A. J. (1991a) *Microbiol. Rev. 55*, 303−315.
Gilkes, N. R., Claeyssens, M., Aebersold, R., Henrissat, B., Meinke, A., Morrison, H. D., Kilburn, D. G., Warren, R. A. J., & Miller, R. C., Jr. (1991b) *Eur. J. Biochem. 202*, 367−377.
Gilkes, N. R., Jervis, E., Henrissat, B., Tekant, B., Miller, R. C., Jr., & Warren, R. A. J. (1992) *J. Biol. Chem. 267*, 6743−6749.
Hei, J. D., & Clark, D. S. (1993) *Biotechnol. Bioeng. 42*, 1245−1251.
Henrissat, B. (1994) *Cellulose 1*, 169−196.
Iwagami, S. G., Creagh, A. L., Haynes, C. A., Borsari, M., Felli, I. C., Piccioli, M., & Eltis, L. D. (1995) *Protein Sci. 4*, 2562−2572.
Jeffries, T. W. (1992) *ACS Symp. Ser. 476*, Chapter 18.
Kempton, J. B., & Withers, S. G. (1992) *Biochemistry 31*, 9961−9969.

Kreimer, D. I., Shnyrov, V. L., Villar, E., Silman, I., & Weiner, L. (1995) *Protein Sci. 4*, 2349−2357.
Leatherbarrow, R. G. (1990) GraFit, Version 2.0, Erithacus Software Ltd., Staines, U.K.
Lee, Y.-E., Lowe, S. E., Henrissat, B., & Zeikus, J. G. (1993) *J. Bacteriol. 175*, 5890−5898.
Liu, Y., & Sturtevant, J. M. (1996) *Biochemistry 35*, 3059−3062.
Miller, R., Jr., Gilkes, N., Johnson, P., Kilburn, D., Kwan, E., Meinke, A., Schmuck, M., Hua, S., Tomme, P., & Warren, A. (1995) Proceedings of Sixth International Conference on Biotechnology in the Pulp and Paper Industry, Vienna, Austria, June 11−15, 1995.
Nikolova, P., Duff, S., MacLeod, A., & Haynes, C. A. (1996) *Ann. N.Y. Acad. Sci. 799*, 19−25.
O'Neill, G., Goh, S. H., Warren, R. A. J., Kilburn, D. G., & Miller, R. C., Jr. (1986) *Gene 44*, 325−330.
Pace, N. C. (1990) *Trends Biochem. Sci. 15*, 14−17.
Privalov, P. L. (1979) *Adv. Protein Chem. 33*, 167−237.
Privalov, P. L. (1989) *Annu. Rev. Biophys. Chem. 18*, 47−69.
Ray, R. R., Jana, S. C., & Nanda, G. (1994) *FEBS Lett. 356*, 30−32.
Ruiz-Arribas, A., Santamaria, R. I., Zhadan, G. G., Villar, E., & Shnyrov, V. L. (1994) *Biochemistry 33*, 13787−13791.
Sanchez-Ruiz, J. M., Lopez-Lacomba, J. L., Cortijo, M., & Mateo, P. L. (1988) *Biochemistry 27*, 1648−1652.
Shortle, D., Wang, Y., Gillespie, J. R., & Wrabl, J. O. (1996) *Protein Sci. 5*, 991−1000.
Sigurskjold, B. W., Svensson, B., Williamson, G., & Driguez, H. (1994) *Eur. J. Biochem. 225*, 133−141.
Tanaka, A., Fukada, H., & Takahashi, K. (1995) *J. Biochem. 117*, 1024−1028.
Terashima, M., Kubo, A., Suzawa, M., Itoh, Y., & Katoh, S. (1994) *Eur. J. Biochem. 226*, 249−254.
Thello-Solis, S. R., & Hernandez-Arana, A. (1995) *Biochem. J. 311*, 969−974.
Tomme, P., Driver, D. P., Amandoron, E. A., Miller, R. C., Jr., Warren, R. A. J., & Kilburn, D. G. (1995) *J. Bacteriol. 177*, 4356−4363.
Tomme, P., Creagh, A. L., Kilburn, D. G., & Haynes, C. A. (1996) *Biochemistry 35*, 13885−13894.
Wakarchuk, W. W., Sung, W. L., Campbell, R. L., Cunningham, A., Watson, D. C., & Yaguchi, M. (1994) *Protein Eng. 7*, 1379−1386.
White, A., Withers, S. G., Gilkes, N. R., & Rose, D. (1994) *Biochemistry 33*, 12546−12552.
Wintrode, P. L., Griko, Y. V., & Privalov, P. L. (1995) *Protein Sci. 4*, 1528−1534.
Xu, G.-Y., Ong, E., Gilkes, N. R., Kilburn, D. G., Muhandiram, D. R., Brandts, M. H., Carver, J. P., Kay, L. E., & Harvey, T. S. (1995) *Biochemistry 34*, 6993−7008.
Yang, S.-T., Marchio, J. L., & Yen, J.-W. (1994) *Biotechnol. Prog. 10*, 525−531.

BI962367F